

## Article

# Disposable Pencil Lead as an Electrochemical Transducer for Monitoring Catechol in River and Tap Water

Farzana Akter<sup>1</sup>, Dulal Chandra Kabiraz<sup>1,\*</sup>, Md. Monirul Islam<sup>1</sup>, Shahed Ahmed<sup>1</sup>, Md. Abu Hanif<sup>2</sup>  
and Young Soon Kim<sup>2</sup>

<sup>1</sup> Department of Chemistry, Faculty of Science, University of Rajshahi, Rajshahi 6205, Bangladesh; farzu.chem.ru@gmail.com (F.A.); monirchem@ru.ac.bd (M.M.I.); shahed.jami007@gmail.com (S.A.)

<sup>2</sup> Institute of Carbon Technology, Jeonju University, Jeonju 55069, Republic of Korea; hanif21@jj.ac.kr (M.A.H.); kyscb@jj.ac.kr (Y.S.K.)

\* Correspondence: dulal.chem@ru.ac.bd

**Abstract:** A cheap and disposable pencil graphite electrode (PGE) was developed by the incorporation of amine groups (Am-PGE-1). A further improvement in the performance was observed when the aminated electrode (Am-PGE-1) was activated by applying a negative potential scan (Am-PGE-2). The electrochemical transport properties were evaluated through cyclic voltammetry (CV) and electrochemical impedance spectroscopy (EIS). The Nyquist plot showed a reduced charge transfer resistance value of 24.3  $\Omega$  for Am-PGE-2, while it was 95.1  $\Omega$  for bare PGE. Thus, Am-PGE-2 was used as a sensing platform for the detection of catechol. It was found that the electrochemical response of catechol oxidation at Am-PGE-2 was twice than the current obtained for bare PGE. Additionally, the effect of pH of the supporting electrolyte and reaction kinetic were studied. The heterogeneous electron transfer rate constant was calculated to be 0.01 s<sup>-1</sup>. Moreover, CV study revealed that the redox reaction of catechol was a quasi-reversible and diffusion-controlled process. The square wave voltammetry (SWV) technique was applied for the quantitative determination of catechol. The peak current showed a linear dependency on the concentration of catechol from 3 to 150  $\mu$ M. Furthermore, the analyte could be detected as low as 3.86  $\mu$ M. Likewise, the sensor demonstrates a good selectivity towards the target analyte than the other possible interfering molecules or ions. Aiming to examine practical applicability, real samples, such as river and household tap water, were tested by using the proposed transducer, and the satisfactory recoveries demonstrate the effectiveness of Am-PGE-2 in real life applications.

**Keywords:** pencil graphite electrode (PGE); amine-functionalization; square wave voltammetry; catechol; river water



**Citation:** Akter, F.; Kabiraz, D.C.; Islam, M.M.; Ahmed, S.; Hanif, M.A.; Kim, Y.S. Disposable Pencil Lead as an Electrochemical Transducer for Monitoring Catechol in River and Tap Water. *Coatings* **2023**, *13*, 913. <https://doi.org/10.3390/coatings13050913>

Academic Editor: Carlo Antonini

Received: 28 March 2023

Revised: 25 April 2023

Accepted: 9 May 2023

Published: 12 May 2023



**Copyright:** © 2023 by the authors. Licensee MDPI, Basel, Switzerland. This article is an open access article distributed under the terms and conditions of the Creative Commons Attribution (CC BY) license (<https://creativecommons.org/licenses/by/4.0/>).

## 1. Introduction

Catechol is known as a dihydroxy benzene isomer, which is largely used as an antioxidant, flavoring agent, medicine, pesticide, etc. The non-bio-degradable isomer comes into the environment from various sources including industrial wastewater, cooking factory, paper mill, pharmaceutical industries, etc. [1]. When parts per million (ppm) levels of concentration accumulate in the human body, catechol causes various anomalous health conditions, such as dermatitis, catarrh, convulsion, and kidney disease [2]. Therefore, the International Agency for Research on Cancer (IARC) has classified catechol in terms of a carcinogenic risk to humans [3]. Furthermore, it has been listed as a priority pollutant by the EPA and the USA [4]. Due to the adverse effects on animal and human health, the detection of catechol has long been an important purpose of analytical chemistry research.

So far, various laboratory-based techniques have been routinely applied to quantify catechol, such as high-performance liquid chromatography (HPLC) [5], gas chromatography-mass spectrophotometry (GC-MS) [6], spectrophotometry [7], electrochemiluminescence [8],

pH-based flow injection analysis [9], etc. However, the above-mentioned techniques are not suitable in terms of point-of-care (POC). Furthermore, these methods are expensive, need organic solvents, have multiple washing steps, require a highly skilled technician, have very narrow limits of detection and are time consuming, etc. [10]. Electro-analytical techniques have been of great interest due to simple instrumentation: showing a high accuracy, sensitivity, short analysis time and cost-effectiveness compared to other methods [11–15].

In the electrochemical analysis of catechol, a glassy carbon electrode (GCE) is widely used [16–19]. To achieve a high sensitivity and selectivity, numerous strategies such as mechanical polishing [20], anodization of GCE [19], applying nanoparticles [18,21], deposition of conducting polymers [17,22], or polymer nanoparticle composites are adopted [23,24]. Although quick response and low limit of detection (LOD) are reported, the success of the modified electrode in practical application is not beyond question, because in the case of modified electrodes, the modifiers might be easily pulled out from the surface and contaminate the solution [25]. This results in a loss of sensitivity, low reproducibility, and poor stability. On the other hand, introducing a functional group, for example, amine groups, directly onto the surface can lead to a possible solution to these problems. The introduction of amino groups was first reported by Uchiyama et al. who used chronoamperometry to introduce amino groups onto the GCE surface in an ammonium carbamate solution [26,27]. The formation of the C-N bond at the glassy carbon surface was verified using X-ray photoelectron spectrophotometry [26]. The introduction of the amino group to the carbon surface was verified using cyclic voltammetry in catechol where an elevated electro-catalytic activity was observed for the modified electrode. It was hypothesized by Pan et al. that the 2p lone-pair electron in an amine group would interact with the graphite through p- $\pi$  conjugation and provide an enhanced electro-catalytic activity [28]. Until now, many scientists have used amino group-incorporated GCE electrodes for detecting urea, nitrite, chlorine, etc. [26,28,29]. However, GCE is expensive and it cannot be discarded even if the electrode becomes fouled. In terms of reuse, tedious surface polishing procedures are needed. In fact, the polishing process requires an organic solvent and a copious amount of water to remove alumina powder from the electrode surface. Furthermore, many modification procedures increase the total cost and the electrodes are not disposable. That is why it is necessary to find an alternative to the conventional electrode.

Considering the low cost and conducting properties of PGE, pencil leads were used as an electrode in 1996 [30]. The environmental friendliness, large commercial availability, and disposal nature of PEGs have helped them to attain significant popularity in an electrochemical sensing platform [15,31]. A large working potential window is also available in comparison to a metallic (Au or Pt) electrode [32]. Furthermore, according to Bond et al. PEGs generate smaller background current compared to GCEs, and noble metal electrodes [33]. Recently various modified PGEs or unmodified PGE-based sensing devices have been reported [31,34–37]. For example, V. Kumar et al. incorporated copper nanoparticles onto the PGE surface and applied the modified electrode for the detection of Adenine. They reported a LOD of 200 nM by using the CV technique [38].

The aim of the present work was to improve electrocatalytic activity of bare PGE by using the amine-functionalization strategy. The aminated pencil graphite electrode (Am-PGE) further cathodised Am-PGE (Am-PGE-2). Thus, it was expected that the oxygen containing groups along with the amine groups may improve catalytic activity of PGE towards catechol. To the best of our knowledge, the electro-oxidation of catechol at Am-PGE-2 has not been reported yet. The square wave voltammetry (SWV) technique was used for the electrochemical quantitation of catechol. Finally, the practical feasibility of Am-PGE-2 was tested in real samples (river and tap water) analysis.

## 2. Materials and Methods

Catechol (1, 2-dihydroxy benzene, 99%) was purchased from HiMedia chemicals (HiMedia, Mumbai, India). Potassium chloride (KCl, 99.9%–100.5%), and calcium chloride (CaCl<sub>2</sub>, 98%) were obtained from Merck (E. Merck India Private Limited, Bengaluru,

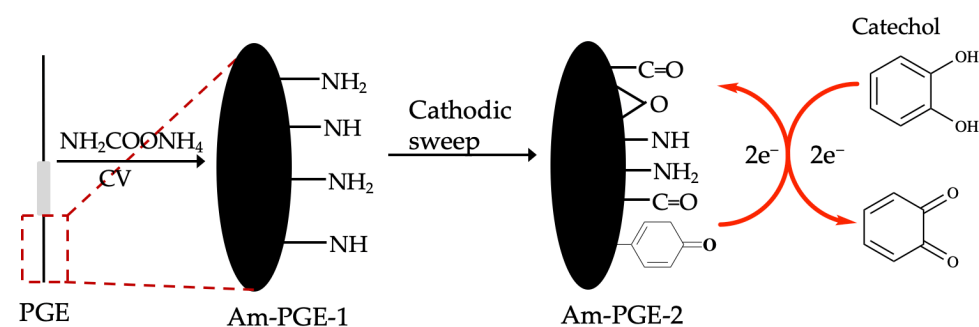
India). Glycine (98.5%), sodium phosphate ( $\text{NaH}_2\text{PO}_4 \cdot 2\text{H}_2\text{O}$ , 98%), and disodium phosphate ( $\text{Na}_2\text{HPO}_4$ , 99%) were bought from Breckland scientific supplies (Stafford, UK). Phenylalanine (99%) and alanine (99%) were collected from Fluka (Mumbai, India), and Thomas Baker (Mumbai, India), respectively. Glucose (99%), and zinc sulfate ( $\text{ZnSO}_4 \cdot 7\text{H}_2\text{O}$ , 99%) were purchased from Fluka (Mumbai, India). Calcium carbonate ( $\text{CaCO}_3$ , 98%) and urea (99%) were collected from Loba (Mumbai, India). Barium nitrate [ $\text{Ba}(\text{NO}_3)_2$ , 99%] was purchased from Timstar laboratory supplies (Stafford, UK). Potassium ferrocyanide [ $\text{K}_4\text{Fe}(\text{CN})_6$ , 98%], and lead chloride ( $\text{PbCl}_2$ , 98%) were brought from Fisher scientific company (Thermo Fisher Scientific Inc., Waltham, MA, USA), respectively. Cadmium chloride ( $\text{CdCl}_2$ , 99%), and potassium ferricyanide [ $\text{K}_3\text{Fe}(\text{CN})_6$ , 98%] were collected from Matheson Colmer and Bell (New Jersey, OH, USA). The HB pencil lead of 0.5 mm diameter was purchased from Kokuyo Camlin Ltd., Mumbai, India.

Electrochemical experiments were performed using an electrochemical workstation of IVIUMSTAT-A 25,313 (Ivium Technologies B.V., Eindhoven, The Netherlands). The electrochemical experiments were carried out by using a conventional electrochemical cell comprised of three electrodes where a pencil graphite electrode (PGE, Am-PGE-1 and Am-PGE-2), a platinum plate, and silver/silver chloride (saturated KCl, CHI 111 Loveland, CO, USA) electrode were used as working, counter, and reference electrode, respectively. The electrochemical cell contained 10 mL of supporting electrolyte and the appropriate amount of catechol. No gas was purged aiming to deaeration. All solutions used in this study were prepared just before the experiments. All aqueous solutions were prepared with ultra-pure ( $18 \Omega$ ) water which was obtained from a Milli-Q water purifying system. For pH adjustment, acidic ( $\text{H}_3\text{PO}_4$ ) and basic ( $\text{NaOH}$ ) solutions were used. All experiments were carried out in an air-conditioned room and the temperature was kept constant ( $25 \text{ }^\circ\text{C} \pm 0.01$ ).

### 3. Results and Discussion

#### 3.1. Preparation and Characterization of Am-PGE

At first, PGE was polished with waterproof abrasive 120 series paper, followed by washing with a copious amount of ultra-pure water. After that, it was sonicated in ultra-pure water for five minutes and finally washed with ultra-pure water. Then, the electrode was electro-oxidized in 0.5 M ammonium carbamate in 0.1 M PBS solution at 1.2 V vs. Ag/AgCl (Sat'd KCl). The amine group that incorporated PGE was named as Am-PGE-1. Next, the Am-PGE-1 was further polarized in PBS at  $-1.0$  V for 15 min at room temperature and termed as Am-PGE-2. The PGE modification strategy is illustrated in Scheme 1.



**Scheme 1.** Schematic of fabrication of Am-PGE-2 and possible reaction mechanism of catechol.

Electrochemical characterizations are useful techniques that are usually used to investigate some vital properties of electrodes, such as electrical conductivity and electrocatalytic features [34]. The BPGE, Am-PGE-1 and Am-PGE-2 electrodes are characterized by CV and EIS measurements. CVs were recorded in 5 mM [ $\text{Fe}(\text{CN})_6$ ] $^{3-/4-}$  in 0.1 M KCl at a scan rate of  $50 \text{ mVs}^{-1}$ . As illustrated in Figure 1a, all CVs exhibit typical features of anodic and cathodic peaks; however, their intensities significantly differ. Therefore, it can be concluded that Am-PGE-2 shows far better electro-catalytic activity than Am-PGE-1 and BPGE.

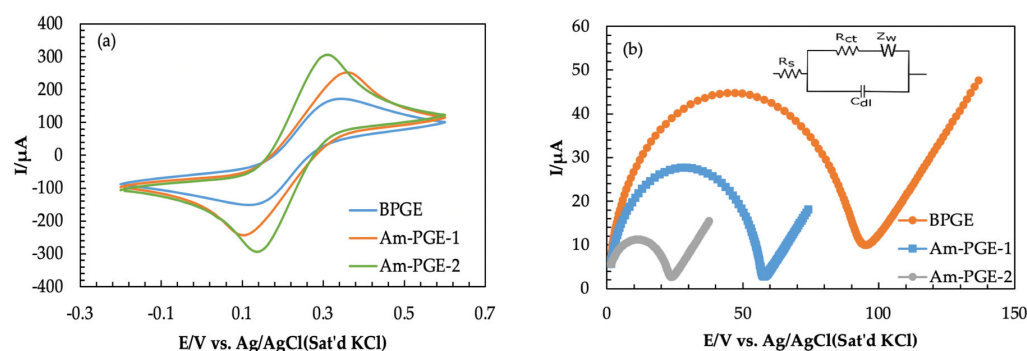


**Figure 1.** (a) Cyclic Voltammograms of 5.0 mM  $\text{Fe}(\text{CN})_6^{3-/4-}$  at BPGE, AmPGE-1, and Am-PGE-2 with scan rate  $50 \text{ mVs}^{-1}$ ; (b) Nyquist plots for three electrodes in 5 mM  $[\text{Fe}(\text{CN})_6]^{3-/4-}$  containing 0.1 M KCl solution [frequency range: 800 kHz to 500 Hz; amplitude: 180 mV].

The electrochemical impedance spectroscopy (EIS) experiment is an important tool that is used for the elucidation of electron transfer kinetics, and the corresponding Nyquist plot is presented as a plot of the real ( $Z'$ ) and imaginary ( $-Z''$ ) aspects [39,40]. The EIS experiment was done by using the same redox couple with a frequency range of 800 kHz to 500 Hz, and the amplitude was 180 mV (Figure 1b). In this study, the Randles circuit was used for simulation, which is provided in the inset of Figure 1b. Randle's circuit consists of electrolyte resistance ( $R_s$ ), electron-transfer resistance ( $R_{ct}$ ), double-layer capacitance ( $C_{dl}$ ), and Warburg impedance ( $Z_W$ ). The Nyquist plot consists of a semi-circular portion and a linear portion; the semi-circular region of the Nyquist plot corresponds to the electron transfer-limited process at higher frequencies, while the linear portions belong to the diffusion-controlled process at lower frequencies. The semi-circular diameter represents the charge transfer resistance ( $R_{ct}$ ) [41,42]. The fall in the value of  $R_{ct}$  indicates the augment in the electro-catalytic performance of the electrode and vice versa. As can be seen from the Nyquist plot, BPGE depicts an enlarged semi-circle with a diameter of  $95.1 \Omega$ , whereas the Am-PGE-1 and Am-PGE-2 show a semi-circle with a reduced diameter of  $58.2$  and  $24.3 \Omega$ . Therefore, the reduced active site shows improved electrocatalytic activity than the oxidized form (Am-PGE-1). This phenomenon can be interpreted as the presence of other functional groups namely  $>C=O$  groups on the surface of Am-PGE-2 along with the amine groups. G. Ilangoan et al. demonstrated that a higher amount of  $>C=O$  at the GCE surface was produced after polarization with negative potential. The existence of carbonyl groups in reduced electrodes was confirmed with the help of XPS analysis [43,44]. The presence of these groups together with amine groups provides a synergistic effect and allows greater adsorption of the analyte. Thus, escalated reaction sites enhance the electrocatalytic activity of the Am-PGE-2 electrode.

### 3.2. The Electrochemical Behavior of Catechol at Am-PGE

The electrochemical behavior of catechol was investigated at bare PGE (BPGE), Am-PGE-1, and Am-PGE-2 using cyclic voltammetry. The electrochemical signals obtained from  $100 \mu\text{M}$  catechol in PBS (0.1 M) are given in Figure 2. The oxidation and reduction peak potentials are 0.39/0.06, 0.22/0.14, and 0.23/0.15 for BPGE, Am-PGE-1, and Am-PGE-2, respectively. The significantly lowered peak potential separation ( $\Delta E_p$ ) of only 80 mV for Am-PGE-1 and Am-PGE-2 manifests faster electron transfer between the analyte and transducer. Furthermore, the peak current also improved about two-fold after the incorporation of amine groups. As expected, the highest signal was observed for Am-PGE-2 among the three tested transducers.

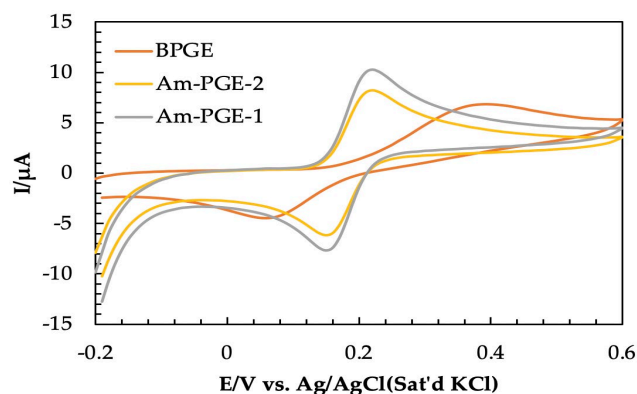


**Figure 2.** Cyclic voltammograms of 100  $\mu\text{M}$  catechol in 0.1 M PBS on BPGC, Am-PGE-1, and Am-PGE-2 at  $50 \text{ mVs}^{-1}$ .

### 3.3. The Active Surface Area

Before using any working electrode, it is necessary to measure the actual surface area. Redox behavior of  $5.0 \text{ mM Fe}^{3-/4-}$  was observed at different scan rates ( $10$  to  $100 \text{ mVs}^{-1}$ ) by using the CV technique, as shown in Figure 3. As can be seen from Figure 3a, the peak current increases with an increasing scan rate. Additionally, the difference in peak potentials ( $\Delta E_p$ ) also increases. This occurred due to the decrease in diffusion layer thickness [37]. The anodic peak currents are also plotted against the square root of the scan rate and illustrated in Figure 3b. From the linear regression equation, the slope was found to be  $0.0005$ . The value of the slope is usually used in the well-established Randles–Sevcik equation [45,46] to calculate the actual surface area. The equation is as follows:

$$I_p = 2.69 \times 10^5 A C n^{3/2} D^{1/2} \nu^{1/2} \quad (1)$$

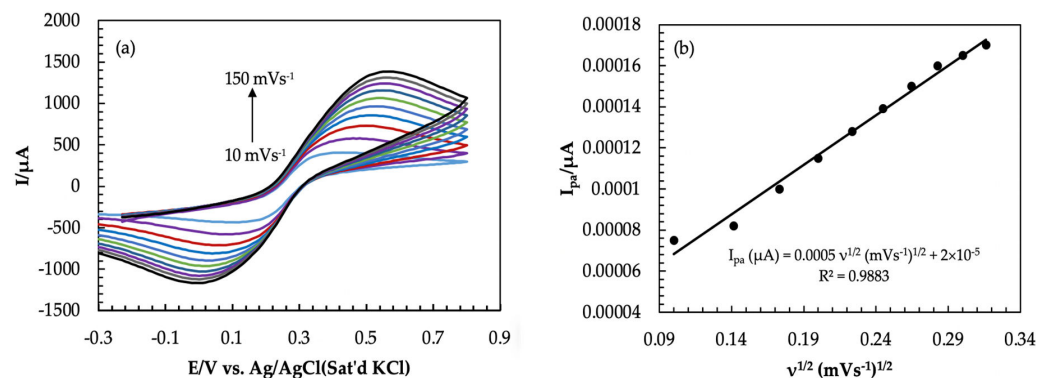


**Figure 3.** (a) Cyclic Voltammograms of  $5.0 \text{ mM Fe(CN)}_6^{3-/4-}$  in 1.0 M KCl at different scan rates (Am-PGE-2); (b) graph of anodic peak current vs. square root of scan rate ( $10$ – $100 \text{ mVs}^{-1}$ ).

The slope of the above equation can be written as:

$$\text{Slope} = 2.69 \times 10^5 A C n^{3/2} D^{1/2} \quad (2)$$

where  $A$  is the actual surface area ( $\text{cm}^2$ ),  $C$  is the concentration of analyte in this experiment concentration,  $\text{Fe}^{3-/4-}$  was  $5 \times 10^{-6} \text{ mol/cm}^3$  (analyte),  $n$  is the number of electrons which value is 1,  $\nu$  is the scan rate ( $\text{Vs}^{-1}$ ), and  $D$  is the diffusion coefficient and its value  $7.6 \times 10^{-6} \text{ cm}^2 \text{ s}^{-1}$  [41]. By putting slope value as well as the value of  $C$ ,  $n$ , and  $D$  in Equation (3), the actual surface area was calculated to be  $0.135 \text{ cm}^2$ , which is smaller than the geometric surface area.

### 3.4. Effect of pH

The effect of the supporting electrolyte pH on the electrochemical behavior was investigated. Six different solutions with a pH range of 4.0 to 9.0 were chosen and CVs were recorded on Am-PGE-2 at a  $50 \text{ mVs}^{-1}$  scan rate. As revealed by Figure 4a, the anodic peak current increases with the increase of the supporting electrolyte's pH up to 7.0, then it follows a decreasing trend as the solution pH is further increased (Figure 4b). This can be explained as attenuation of the proton taking part in the electrochemical reaction, and as a result, catechol produces a high overpotential at low pH because it would not be ionized [47]. Due to a shortage of protons in the solution at a pH value greater than 7.0, the electrochemical reaction becomes more difficult. Catechol can be easily turned into anions in high pH solution, giving rise to the electrostatic repulsion between the two dihydroxy benzene isomers, which would make the peak current decrease [48]. Since the maximum peak current was obtained at pH 7.0, this was chosen as the optimum pH value for the electrochemical detection of catechol.

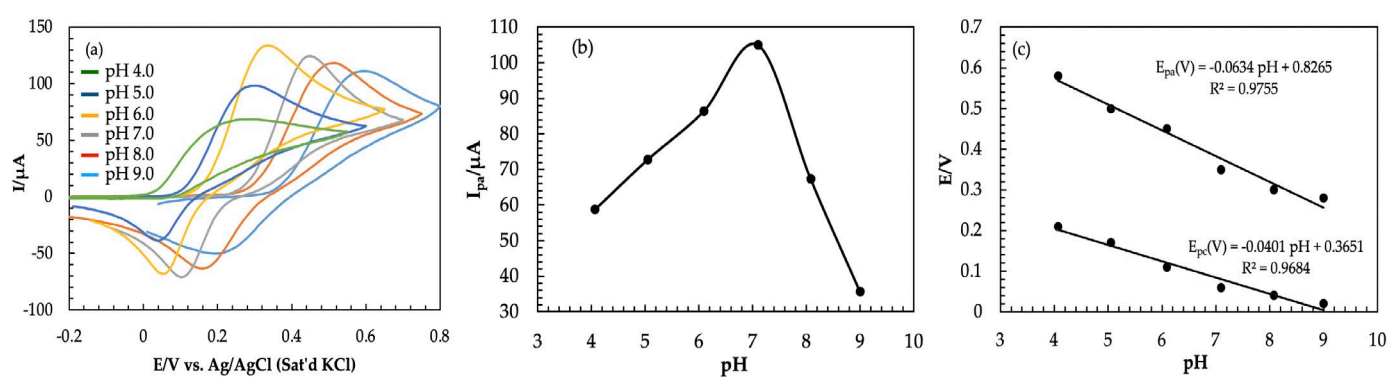


**Figure 4.** (a) Cyclic Voltammograms of 2.0 mM of catechol in 0.1 M PBS at different pH values (pH = 4.0–9.0); (b) the relationship between the pH values (4.0–9.0) and anodic peak current at scan rate  $50 \text{ mVs}^{-1}$ ; (c) effect of pH on peak potential.

The relationship between peak potential and pH was also investigated, as shown in Figure 4c. Two linear relationships were obtained with the regression equations of  $E_{pa}(\text{V}) = -0.0634 \text{ pH} + 0.8265$  ( $R^2 = 0.9755$ ) for the oxidation potential, and  $E_{pc}(\text{V}) = -0.0401 \text{ pH} + 0.36551$  ( $R^2 = 0.9684$ ) for the reduction potential. Oxidation potential shifted to more negative values when pH increased, which indicated that the proton transfer process was involved in the oxidation of catechol. It is reported that the slope value close to  $58.5 \text{ mV pH}^{-1}$  indicates a two-electrons and protons process of the electrochemical reaction [49]. Herein, the calibration curve of E vs. pH, in the pH range of 4.0 to 9.0 have the slope values of  $63.4 \text{ mV pH}^{-1}$  and  $40.1 \text{ mV pH}^{-1}$ . Therefore, the slopes of the two regression equations are approximate to the theoretical value of  $58.5 \text{ mV pH}^{-1}$ , which implies that two electrons and protons are associated here.

### 3.5. Effect of Scan Rate on Am-PGE-2 Surface

The effect of the scan rate on the peak current and peak potential at Am-PGE-2 in a 2.0 mM catechol in 0.1 M phosphate buffer solution (pH = 7.0) was investigated by using the CV technique which was demonstrated in Figure 5. With an increasing scan rate from 10 to  $80 \text{ mVs}^{-1}$ , all redox peak current increases. Additionally, the anodic ( $E_{pa}$ ) and cathodic peak potentials ( $E_{pc}$ ) are shifted to a positive direction and reduction peak potential shifted to a negative potential, i.e.,  $E_p$  is dependent on  $v$ . In addition, the peak current ratio is not unified. Therefore, it was concluded that the catechol reaction on the Am-PGE-2 surface is a quasi-reversible reaction.

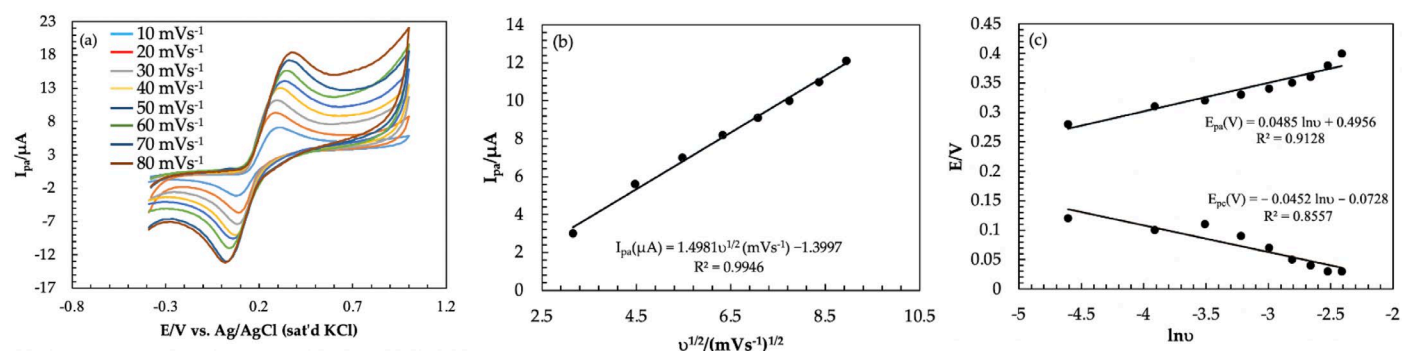


**Figure 5.** (a) Effect of scan rate of 2 mM catechol in PBS at scan rate of 10 to 90  $\text{mVs}^{-1}$ ; (b) Graph of anodic peak current vs. scan rate; (c) Effect of scan rate on peak potentials.

The oxidation peak currents ( $I_{pa}$ ) are proportional to the square root of the scan rate ( $v^{1/2}$ ) (Figure 5b) indicating that the redox reaction of catechol is a diffusion-controlled process. The number of electrons associated with the redox reaction can be calculated from the slope value of  $E_p$  vs.  $\ln v$ , which was represented in Figure 5c, as proposed by Laviron's theory [50]. The slopes are  $\frac{2.3RT}{(1-\alpha)nF}$  and  $-\frac{2.3RT}{\alpha nF}$  (where,  $R$  is the molar gas constant,  $T$  is the absolute temperature,  $n$  is the number of electron involved in an electrode reaction, and  $F$  is the Faraday constant) for anodic and cathodic reaction, respectively, where  $\alpha$ , the electron transfer coefficient for catechol at Am-PGE-2, can be calculated using the following equation:

$$\log K_a/K_c = \log \alpha/(1 - \alpha) \quad (3)$$

The linear regression equations for anodic potential;  $E_{pa} = 0.0485 \ln v + 0.4956$  ( $R^2 = 0.9128$ ) and cathodic potential;  $E_{pc} = -0.0452 \ln v - 0.0728$  ( $R^2 = 0.86$ ) were obtained from the plot of  $E_p$  vs.  $\ln v$ .  $K_a$ , and  $K_c$  (value of Slope) were obtained from a plot of  $E_{pa}$  vs.  $\ln v$  and  $E_{pc}$  vs.  $\ln v$ , respectively. Putting values of  $K_a$  (0.0485) and  $K_c$  (0.0452) in Equation (3),  $\alpha$  was calculated to be 0.51. Finally, the number of electrons associated in the chemical reaction was estimated by using  $\alpha$ ,  $R$ ,  $T$ , and value of slope. The number of electrons was calculated to be two. This result also supports that the redox reaction of catechol is a two-electron and two-proton process.

In electrochemistry, the estimation of the heterogeneous electron transfer rate constant ( $k_s$ ) is of paramount interest when the performance of electrode materials is examined. The value of the rate constant provides an indication of the speed of electron transfer between an electroactive species and an electrode surface. The heterogeneous electron-transfer rate constant ( $k_s$ ) can also be obtained using the following equation [34]:

$$\text{Log } k_s = \alpha \text{Log}(1 - \alpha) + (1 - \alpha) \text{Log} \alpha - \text{Log} \left( \frac{RT}{nFv} \right) - \frac{\alpha(1 - \alpha)nF\Delta E_p}{2.3RT} \quad (4)$$

where  $\alpha$  is the electron transfer coefficient,  $n$  is the number of the electron involved in an electrode reaction,  $F$  is the Faraday constant,  $v$  is the scan rate,  $R$  is the molar gas constant, and  $T$  is the absolute temperature. The heterogeneous electron transfer rate constant for catechol on Am-PGE-2 was estimated to be  $0.01 \text{ s}^{-1}$ . J. Peng et al. reported that the rate constant for Catechol on the GCE surface was found to be  $1.65 \times 10^{-3} \text{ s}^{-1}$  [51].

### 3.6. Calibration Curve

The variation of peak current with the concentration of catechol at the Am-PGE-2 surface was observed by the SWV technique. From Figure 6a, it can be seen that the peak current of catechol is proportionally increased from 3 to 150  $\mu\text{M}$ . The plot of peak current vs. concentration of catechol appears in a linear relationship with regression equation  $I_{pa} (\mu\text{A})$

= 0.0413 ( $\mu\text{M}$ ) + 0.0774 with co-relation coefficient  $R^2 = 0.9932$ . The limit of detection (LOD) and limit of quantification (LOQ) were calculated by using Equations (5) and (6) [41]:

$$\text{LOD} = 3 S/M \quad (5)$$

$$\text{LOQ} = 10 S/M \quad (6)$$

where  $S$  is the standard deviation and  $M$  is the slope of the calibration plots. The values of LOD and LOQ were estimated to be 3.86 and 6.53  $\mu\text{M}$ , respectively. To show the advantage of the proposed electrode on the quantification of catechol, these values are comparable with values reported by some previously published work and summarized in Table 1. As can be seen from Table 1, the analytical performance of the developed electrode is competitive with the previously reported catechol detection.

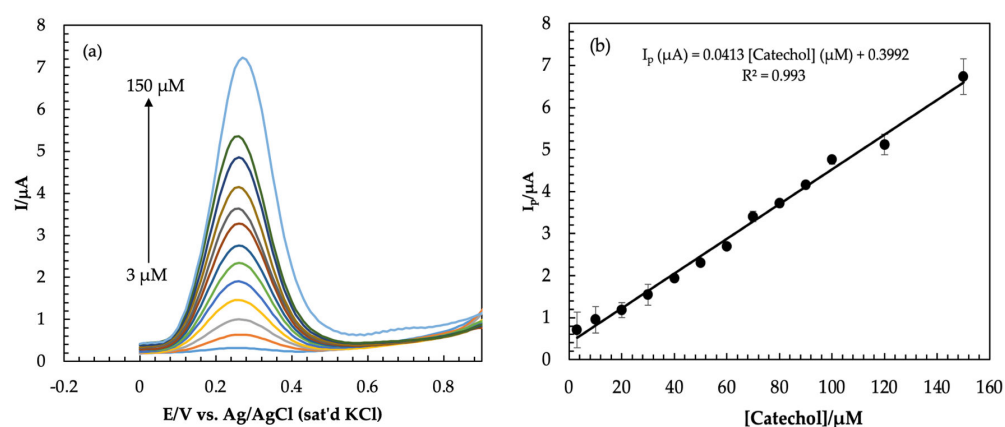


**Figure 6.** (a) Square wave voltammograms of catechol in 0.1 M PBS solution of pH = 7.0 on Am-PGE-2 surface with different concentrations; (b) graph of anodic peak current vs. concentration of catechol.

**Table 1.** Comparison of the prepared sensor with others for the detection of catechol.

Modified Electrode	Technique	Linearity/ $\mu\text{M}$	LOD/ $\mu\text{M}$	LOQ/ $\mu\text{M}$	Ref.
DL-methionine/CPE	CV	20.66–209.9	55.66	185.5	[45]
3-Thiophenemalonic acid/GCE	DPV	7.81–500	7.81		[52]
Silosesquioxane/CPE	DPV	10–300	10		[53]
Zn/Al layered double hydroxide film/GCE	DPV	3–1.5	9.0		[54]
malachite green/multi-wall carbon tube/GCE	DPV	30–1190	5.8		[55]
[Cu(Sal- $\beta$ -Ala)(3,5-DMPz)]/SWCNTs/GCE	DPV	5–215	3.5		[56]
Am-PGE-2	SWV	3–150	3.86	6.53	This work

### 3.7. Interference Study

The selectivity of the Am-PGE-2 transducer was examined by the addition of some interfering species in a solution of 100  $\mu\text{M}$  catechol in 0.1 M PBS (pH = 7.0). The overall summary of the interference studies is shown in Figure 7. The results indicated that 1 mM alanine, phenylalanine, glycine, glucose, urea, as well as a great number of cations and anions (10-fold), such as  $\text{Na}^+$ ,  $\text{K}^+$ ,  $\text{Zn}^{2+}$ ,  $\text{Ba}^{2+}$ ,  $\text{Ca}^{2+}$ ,  $\text{Cl}^-$ ,  $\text{SO}_4^{2-}$ ,  $\text{NO}_3^-$ ,  $\text{Pd}^{2+}$ , and  $\text{Cd}^{2+}$  were not interfered. The obtained results were compared with the result of 100  $\mu\text{M}$  catechol in the absence of the interfering agent. The variation in current caused by the interference



species is less than 8% (except phenylalanine). The results reveal that the sensor possesses appreciable anti-interference properties in the presence of these substances.

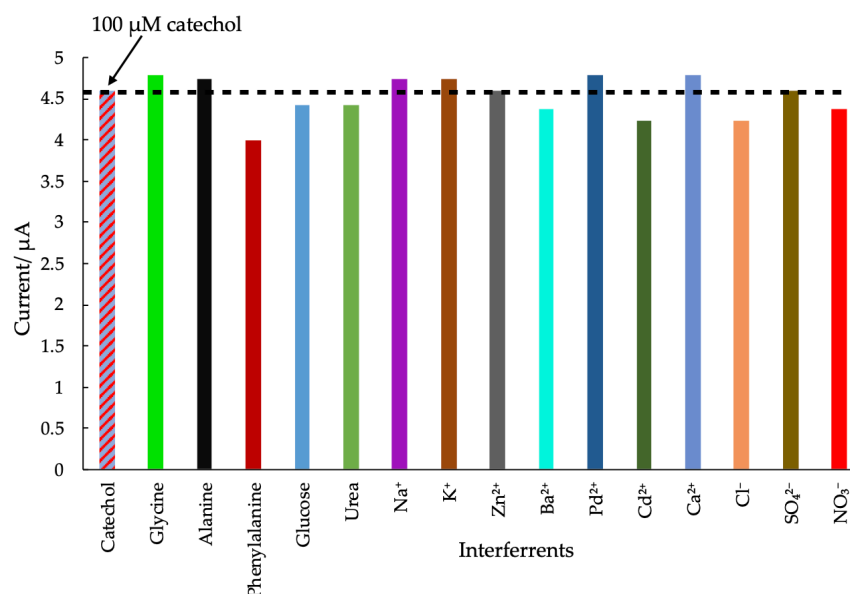


**Figure 7.** Peak variation of 100 μM CC and the different interfering agents such as (1 mM) glycine, alanine, phenylalanine, glucose, urea and 10 fold of KCl, K<sub>2</sub>SO<sub>4</sub>, NaCl, CaCl<sub>2</sub>, ZnSO<sub>4</sub>, PbCl<sub>2</sub>, CdCl<sub>2</sub> and Ba(NO<sub>3</sub>)<sub>2</sub>.

### 3.8. Real Sample Analysis

The applicability of Am-PGE-2 in real sample analysis was explored in environmental water samples, i.e., river water and household tap water. A different concentration of catechol was added in single-step filtered water. The square wave voltammograms were then recorded and catechol concentration was determined using the constructed calibration plot. The results are summarized in Table 2. All measurements were carried out three times under the same conditions. The recoveries of catechol in local tap and river water are 82%–97% and 98%–102%, respectively. Moreover, the average recovery was 94.7%. As can be seen from Table 2, the relative standard deviation (RSD) for each sample analysis is at a level not exceeding 5%, which indicates practical applicability and good accuracy of Am-PGE-2 for the detection of catechol in real samples.

**Table 2.** Recovery of catechol in the real sample (tap and river water).

Sample	Added CC/μM	Found CC/μM (n = 3)	Recovery/%
Tap water	60	49 (± 0.94)	82 (± 1.41)
	30	29 (± 0.64)	97 (± 1.50)
River water	50	49 (± 0.47)	98 (± 0.94)
	100	102 (± 5.12)	102 (± 5.09)

## 4. Conclusions

In this study, a cost-effective PGE was developed by the incorporation of amine groups. The electrode was further activated (Am-PGE-2) by sweeping at negative potential. The EIS data revealed that the Am-PGE-2 shows excellent electrocatalytic activity compared to the bare one, due to the introduction of amine groups and oxygen containing functional groups. The Am-PGE-2 was employed as an electrochemical transducer for the detection of catechol and a two-fold higher signal was achieved compared to the bare one. From the CV study, it was found that the redox behavior of catechol on the Am-PGE-2 surface was a quasi-reversible and diffusion-controlled reaction. In the SWV technique, the current

response for catechol varied in linearity with the concentration range of 3 to 150  $\mu\text{M}$  with a detection limit of 3.86  $\mu\text{M}$ . Apart from this, an anti-interface ability of the electrode surface for the detection of catechol was also observed. Furthermore, it was found that this electrode was able to detect catechol in household tap and river water samples and spiked with different concentrations of catechol with an average recovery rate of 95%, showing its promising application in real sample monitoring without any observation of the matrix effect.

**Author Contributions:** Conceptualization, D.C.K.; methodology, F.A. and D.C.K.; software, M.M.I.; formal analysis, F.A., S.A., M.M.I., M.A.H., Y.S.K. and D.C.K.; investigation, F.A.; data curation, F.A. and S.A.; writing—original draft preparation, F.A., S.A. and D.C.K.; writing—review and editing, M.A.H. and D.C.K.; visualization, M.M.I., M.A.H., Y.S.K. and D.C.K.; supervision, D.C.K.; project administration, D.C.K. All authors have read and agreed to the published version of the manuscript.

**Funding:** The research was supported by the Department of Chemistry, University of Rajshahi, Bangladesh.

**Institutional Review Board Statement:** Not applicable.

**Informed Consent Statement:** Not applicable.

**Data Availability Statement:** Not applicable.

**Acknowledgments:** The authors wish to express gratitude to the Department of Chemistry and the Faculty of Science at the University of Rajshahi, Bangladesh, for providing chemicals and laboratory facilities.

**Conflicts of Interest:** The authors declare no conflict of interest.

## References

1. Mia, M.A.H.; Motin, M.A.; Huque, E.M. Electrochemical oxidation of catechol in the presence of L-Lysine at different pH. *Russ. J. Electrochem.* **2019**, *55*, 370–380. [[CrossRef](#)]
2. Enguita, F.J.; Leitão, A.L. Hydroquinone: Environmental pollution, toxicity, and microbial answers. *Biomed Res. Int.* **2013**, *2013*, 542168. [[CrossRef](#)] [[PubMed](#)]
3. Ghoreishi, S.M.; Behpour, M.; Hajisadeghian, E.; Golestaneh, M. Electrochemical determination of acetaminophen at the surface of a glassy carbon electrode modified with multi-walled carbon nanotube. *J. Chil. Chem. Soc.* **2013**, *58*, 1513–1516. [[CrossRef](#)]
4. Wang, M.; Li, X.; Liu, J.; Xu, W.; Dong, Y.; Liu, P.; Zhang, C. Electrochemically reduced graphene oxide as modified electrode material for determination of dihydroxybenzenes. *J. Wuhan Univ. Technol. Mater. Sci. Ed.* **2017**, *32*, 1220–1224. [[CrossRef](#)]
5. Lee, B.L.; Ong, H.Y.; Shi, C.Y.; Ong, C.N. Simultaneous determination of hydroquinone, catechol and phenol in urine using high-performance liquid chromatography with fluorimetric detection. *J. Chromatogr. B Biomed. Sci. Appl.* **1993**, *619*, 259–266. [[CrossRef](#)]
6. O'Grodnick, J.S.; Dupre, G.D.; Gulizia, B.J.; Blake, S.H. Determination of benzene, phenol, catechol, and hydroquinone in whole blood of rats and mice. *J. Chromatogr. Sci.* **1983**, *21*, 289–292. [[CrossRef](#)]
7. Mohammed, D.H.; Omar, F.K. Spectrophotometric determination of catechol and resorcinol by oxidative coupling with 2,4-dinitrophenyl hydrazine. *Egypt. J. Chem.* **2021**, *64*, 5061–5065. [[CrossRef](#)]
8. Zhao, L.; Lv, B.; Yuan, H.; Zhou, Z.; Xiao, D. A sensitive chemiluminescence method for determination of hydroquinone and catechol. *Sensors* **2007**, *7*, 578–588. [[CrossRef](#)]
9. Sun, Y.; Cui, H.; Li, Y.; Lin, X. Determination of some catechol derivatives by a flow injection electrochemiluminescent inhibition method. *Talanta* **2000**, *53*, 661–666. [[CrossRef](#)]
10. Pistonesi, M.F.; Di Nezio, M.S.; Centurión, M.E.; Palomeque, M.E.; Lista, A.G.; Fernández Band, B.S. Determination of phenol, resorcinol and hydroquinone in air samples by synchronous fluorescence using partial least-squares (PLS). *Talanta* **2006**, *69*, 1265–1268. [[CrossRef](#)]
11. Shashikumara, J.K.; Kumara Swamy, B.E.; Sharma, S.C. A simple sensing approach for the determination of dopamine by poly (Yellow PX4R) pencil graphite electrode. *Chem. Data Collect.* **2020**, *27*, 100366. [[CrossRef](#)]
12. Ali, M.F.B.; Abdel-Aal, F.A.M. In Situ polymerization and FT-IR characterization of poly-glycine on pencil graphite electrode for sensitive determination of anti-emetic drug, granisetron in injections and human plasma. *RSC Adv.* **2019**, *9*, 4325–4335. [[CrossRef](#)] [[PubMed](#)]
13. Rouhollahi, A.; Kouchaki, M.; Seidi, S. Electrically stimulated liquid phase microextraction combined with differential pulse voltammetry: A new and efficient design for In Situ determination of clozapine from complicated matrices. *RSC Adv.* **2016**, *6*, 12943–12952. [[CrossRef](#)]

14. Vishnu, N.; Gandhi, M.; Badhulika, S.; Kumar, A.S. Tea quality testing using 6B pencil lead as an electrochemical sensor. *Anal. Methods* **2018**, *10*, 2327–2336. [[CrossRef](#)]
15. David, I.G.; Popa, D.E.; Buleandra, M.; Moldovan, Z.; Iorgulescu, E.E.; Badea, I.A. Cheap pencil graphite electrodes for rapid voltammetric determination of chlorogenic acid in dietary supplements. *Anal. Methods* **2016**, *8*, 6537–6544. [[CrossRef](#)]
16. Wei, C.; Huang, Q.; Hu, S.; Zhang, H.; Zhang, W.; Wang, Z.; Zhu, M.; Dai, P.; Huang, L. Simultaneous electrochemical determination of hydroquinone, catechol and resorcinol at nafion/multi-walled carbon nanotubes/carbon dots/multi-walled carbon nanotubes modified glassy carbon electrode. *Electrochim. Acta* **2014**, *149*, 237–244. [[CrossRef](#)]
17. Zhang, M.; Ge, C.Y.; Jin, Y.F.; Hu, L.B.; Mo, H.Z.; Li, X.B.; Zhang, H. Sensitive and simultaneous determination of hydroquinone and catechol in water using an anodized glassy carbon electrode with polymerized 2-(Phenylazo) chromotropic Acid. *J. Chem.* **2019**, *2019*, 2327064. [[CrossRef](#)]
18. Zhang, Y.; Xiao, S.; Xie, J.; Yang, Z.; Pang, P.; Gao, Y. Simultaneous electrochemical determination of catechol and hydroquinone based on graphene-TiO<sub>2</sub> nanocomposite modified glassy carbon electrode. *Sens. Actuators B Chem.* **2014**, *204*, 102–108. [[CrossRef](#)]
19. Sunil Kumar Naik, T.S.; Kumara Swamy, B.E. Pre-treated glassy carbon electrode sensor for catechol: A voltammetric study. *J. Electroanal. Chem.* **2018**, *826*, 23–28. [[CrossRef](#)]
20. Kiema, G.K.; Aktay, M.; McDermott, M.T. Preparation of reproducible glassy carbon electrodes by removal of polishing impurities. *J. Electroanal. Chem.* **2003**, *540*, 7–15. [[CrossRef](#)]
21. Goulart, L.A.; Mascaro, L.H. GC electrode modified with carbon nanotubes and NiO for the simultaneous determination of bisphenol A, hydroquinone and catechol. *Electrochim. Acta* **2016**, *196*, 48–55. [[CrossRef](#)]
22. Wang, R.; Wang, S.; Qin, C.; Nie, Q.; Luo, Y.; Qin, Q.P.; Wang, R.; Liu, B.; Luo, D. An electrochemical sensor based on electropolymerization of b-Cyclodextrin on glassy carbon electrode for the determination of fenitrothion. *Sensors* **2023**, *23*, 435. [[CrossRef](#)] [[PubMed](#)]
23. Raj, M.; Gupta, P.; Goyal, R.N.; Shim, Y.B. Graphene/conducting polymer nano-composite loaded screen printed carbon sensor for simultaneous determination of dopamine and 5-hydroxytryptamine. *Sens. Actuators B Chem.* **2017**, *239*, 993–1002. [[CrossRef](#)]
24. Mazloum-Ardakani, M.; Sheikh-Mohseni, M.A.; Benvidi, A. Electropolymerization of thin film conducting polymer and its application for simultaneous determination of ascorbic acid, dopamine and uric acid. *Electroanalysis* **2011**, *23*, 2822–2831. [[CrossRef](#)]
25. Sajid, M.; Baig, N.; Alhooshani, K. Chemically modified electrodes for electrochemical detection of dopamine: Challenges and opportunities. *TrAC—Trends Anal. Chem.* **2019**, *118*, 368–385. [[CrossRef](#)]
26. Uchiyama, S.; Watanabe, H.; Yamazaki, H.; Kanazawa, A.; Hamana, H.; Okabe, Y. Electrochemical introduction of amino group to a glassy carbon surface by the electrolysis of carbamic acid. *J. Electrochem. Soc.* **2007**, *154*, F31. [[CrossRef](#)]
27. Wang, X.; Cao, T.; Zuo, Q.; Wu, S.; Uchiyama, S.; Matsuura, H. Sensitive nitrite detection using a simple electrochemically aminated glassy carbon electrode. *Anal. Methods* **2016**, *8*, 3445–3449. [[CrossRef](#)]
28. Pan, S.; Deen, M.J.; Ghosh, R. Low-cost graphite-based free chlorine sensor. *Anal. Chem.* **2015**, *87*, 10734–10737. [[CrossRef](#)]
29. Wang, X.; Watanabe, H.; Sekioka, N.; Hamana, H.; Uchiyama, S. Amperometric urea biosensor using aminated glassy carbon electrode covered with urease immobilized carbon sheet, based on the electrode oxidation of carbamic acid. *Electroanalysis* **2007**, *19*, 1300–1306. [[CrossRef](#)]
30. David, I.G.; Popa, D.; Buleandra, M. Pencil graphite electrodes: A versatile tool in electroanalysis. *J. Anal. Methods Chem.* **2017**, *2017*, 1905968. [[CrossRef](#)]
31. Yaman, Y.T.; Abaci, S. Sensitive adsorptive voltammetric method for determination of bisphenol A by gold nanoparticle/polyvinyl pyrrolidone-modified pencil graphite electrode. *Sensors* **2016**, *16*, 756. [[CrossRef](#)] [[PubMed](#)]
32. Aoki, K.; Okamoto, T.; Kaneko, H.; Nozaki, K.; Negishi, A. Applicability of graphite reinforcement carbon used as the lead of a mechanical pencil to voltammetric electrodes. *J. Electroanal. Chem.* **1989**, *263*, 323–331. [[CrossRef](#)]
33. Bond, A.M.; Mahon, P.J.; Schiewe, J.; Vicente-Beckett, V. An inexpensive and renewable pencil: Electrode for use in field-based stripping voltammetry. *Anal. Chim. Acta* **1997**, *345*, 67–74. [[CrossRef](#)]
34. Senturk, H.; Eksin, E.; Zeybek, U.; Erdem, A. Detection of senecionine in dietary sources by single-use electrochemical sensor. *Micromachines* **2021**, *12*, 1585. [[CrossRef](#)] [[PubMed](#)]
35. Sree, V.G.; Sohn, J.I.; Im, H. Pre-anodized graphite pencil electrode coated with a poly(Thionine) film for simultaneous sensing of 3-Nitrophenol and 4-Nitrophenol in environmental water samples. *Sensors* **2022**, *22*, 1151. [[CrossRef](#)]
36. Lu, J.Y.; Yu, Y.S.; Chen, T.B.; Chang, C.F.; Tamulevičius, S.; Erts, D.; Wu, K.C.W.; Gu, Y. Fabrication of an extremely cheap Poly(3,4-ethylenedioxythiophene) modified pencil lead electrode for effective hydroquinone sensing. *Polymers* **2021**, *13*, 343. [[CrossRef](#)]
37. Li, Y.; Zhang, J.; Lv, M.; Bai, Y.; Weng, X.; You, C.; Liu, Z. Voltammetric determination of 5-hydroxymethyl-2-furfural in processed cheese using an easy-made and economic integrated 3D graphene-like electrode. *Sensors* **2021**, *22*, 64. [[CrossRef](#)]
38. Kumar, V.; Irnkova, L. Copper nanoparticle modified pencil graphite electrode for electroanalysis of adenine. *Electroanalysis* **2016**, *28*, 2834–2840. [[CrossRef](#)]
39. He, Q.; Liu, J.; Liu, X.; Li, G.; Chen, D.; Deng, P.; Liang, J. A promising sensing platform toward dopamine using MnO<sub>2</sub> nanowires/electro-reduced graphene oxide composites. *Electrochim. Acta* **2019**, *296*, 683–692. [[CrossRef](#)]

40. He, Q.; Liu, J.; Liu, X.; Li, G.; Deng, P.; Liang, J. Manganese dioxide nanorods/electrochemically reduced graphene oxide nanocomposites modified electrodes for cost-effective and ultrasensitive detection of amaranth. *Colloids Surf. B Biointerfaces* **2018**, *172*, 565–572. [[CrossRef](#)]
41. Wan, X.; Yang, S.; Cai, Z.; He, Q.; Ye, Y.; Xia, Y.; Li, G.; Liu, J. Facile synthesis of MnO<sub>2</sub> nanoflowers/N-doped reduced graphene oxide composite and its application for simultaneous determination of dopamine and uric acid. *Nanomaterials* **2019**, *9*, 847. [[CrossRef](#)] [[PubMed](#)]
42. Begum, H.; Ahmed, M.S.; Jeon, S. New approach for porous chitosan-graphene matrix preparation through enhanced amidation for synergic detection of dopamine and uric acid. *ACS Omega* **2017**, *2*, 3043–3054. [[CrossRef](#)] [[PubMed](#)]
43. Ilangovan, G.; Pillai, K.C. Unusual activation of glassy carbon electrodes for enhanced adsorption of monomeric molybdate(VI). *J. Electroanal. Chem.* **1997**, *431*, 11–14. [[CrossRef](#)]
44. Ilangovan, G.; Pillai, K.C. Electrochemical and XPS characterization of glassy carbon electrode surface effects on the preparation of a monomeric molybdate(VI)-modified electrode. *Langmuir* **1997**, *13*, 566–575. [[CrossRef](#)]
45. Baig, N.; Kawde, A.N.; Elgamouz, A.; Morsy, M.; Abdelfattah, A.M.; Othaman, R. Graphene nanosheet-sandwiched platinum nanoparticles deposited on a graphite pencil electrode as an ultrasensitive sensor for dopamine. *RSC Adv.* **2022**, *12*, 2057–2067. [[CrossRef](#)]
46. Liu, S.; Yan, J.; He, G.; Zhong, D.; Chen, J.; Shi, L.; Zhou, X.; Jiang, H. Layer-by-layer assembled multilayer films of reduced graphene oxide/gold nanoparticles for the electrochemical detection of dopamine. *J. Electroanal. Chem.* **2012**, *672*, 40–44. [[CrossRef](#)]
47. Yuan, X.; Yuan, D.; Zeng, F.; Zou, W.; Tzorbatzoglou, F. Preparation of graphitic mesoporous carbon for the simultaneous detection of hydroquinone and catechol. *Appl. Catal. B Environ.* **2013**, *129*, 367–374. [[CrossRef](#)]
48. Zhang, C.; Zeng, L.; Zhu, X.; Yu, C.; Zuo, X.; Xiao, X.; Nan, J. Electrocatalytic oxidation and simultaneous determination of catechol and hydroquinone at a novel carbon nano-fragment modified glassy carbon electrode. *Anal. Methods* **2013**, *5*, 2203–2208. [[CrossRef](#)]
49. Guo, Q.; Huang, J.; Chen, P.; Liu, Y.; Hou, H.; You, T. Simultaneous determination of catechol and hydroquinone using electrospun carbon nanofibers modified electrode. *Sens. Actuators B Chem.* **2012**, *163*, 179–185. [[CrossRef](#)]
50. Laviron, E. General expression of the linear potential sweep voltammogram in the case of diffusionless electrochemical systems. *J. Electroanal. Chem.* **1979**, *101*, 19–28. [[CrossRef](#)]
51. Peng, J.; Gao, Z.N. Influence of micelles on the electrochemical behaviors of catechol and hydroquinone and their simultaneous determination. *Anal. Bioanal. Chem.* **2006**, *384*, 1525–1532. [[CrossRef](#)] [[PubMed](#)]
52. Dorraji, P.S.; Jalali, F. A nanocomposite of poly(melamine) and electrochemically reduced graphene oxide decorated with Cu nanoparticles: Application to simultaneous determination of hydroquinone and catechol. *J. Electrochem. Soc.* **2015**, *162*, B237–B244. [[CrossRef](#)]
53. Silva, P.S.; Gasparini, B.S.; Magosso, H.A.; Spinelli, A. Electrochemical behavior of hydroquinone and catechol at a silsesquioxane-modified carbon paste electrode. *J. Braz. Chem. Soc.* **2013**, *24*, 695–699. [[CrossRef](#)]
54. Li, M.; Ni, F.; Wang, Y.; Xu, S.; Zhang, D.; Chen, S.; Wang, L. Sensitive and facile determination of catechol and hydroquinone simultaneously under coexistence of resorcinol with a Zn/Al layered double hydroxide film modified glassy carbon electrode. *Electroanalysis* **2009**, *21*, 1521–1526. [[CrossRef](#)]
55. Umasankar, Y.; Periasamy, A.P.; Chen, S.M. Electrocatalysis and simultaneous determination of catechol and quinol by poly(malachite green) coated multiwalled carbon nanotube film. *Anal. Biochem.* **2011**, *411*, 71–79. [[CrossRef](#)]
56. Alshahrani, L.A.; Li, X.; Luo, H.; Yang, L.; Wang, M.; Yan, S.; Liu, P.; Yang, Y.; Li, Q. The simultaneous electrochemical detection of catechol and hydroquinone with [Cu(Sal-β-Ala)(3,5-DMPz)<sub>2</sub>]/SWCNTs/GCE. *Sensors* **2014**, *14*, 22274–22284. [[CrossRef](#)]

**Disclaimer/Publisher’s Note:** The statements, opinions and data contained in all publications are solely those of the individual author(s) and contributor(s) and not of MDPI and/or the editor(s). MDPI and/or the editor(s) disclaim responsibility for any injury to people or property resulting from any ideas, methods, instructions or products referred to in the content.